

See discussions, stats, and author profiles for this publication at: <https://www.researchgate.net/publication/10951173>

Counterion-Dependent Excitonic Spectra of Tetra(p -carboxyphenyl)porphyrin Aggregates in Acidic Aqueous Solution

ARTICLE *in* JOURNAL OF THE AMERICAN CHEMICAL SOCIETY · FEBRUARY 2003

Impact Factor: 12.11 · DOI: 10.1021/ja0274397 · Source: PubMed

CITATIONS

108

READS

86

4 AUTHORS, INCLUDING:



[Mark Adam Webb](#)

Canadian Light Source Inc. (CLS)

15 PUBLICATIONS 322 CITATIONS

SEE PROFILE

Counterion-Dependent Excitonic Spectra of Tetra(*p*-carboxyphenyl)porphyrin Aggregates in Acidic Aqueous Solution

Myong Yong Choi, Jennifer A. Pollard, M. Adam Webb, and Jeanne L. McHale*

Contribution from the Department of Chemistry, University of Idaho, Moscow, Idaho 83844-2343

Received June 24, 2002; E-mail: jmchale@uidaho.edu

Abstract: Aggregates of the diacid form of tetra(*p*-carboxyphenyl)porphyrin (TCPP) are found to be stabilized in aqueous solution at low pH in the presence of poly(vinyl alcohol). At pH values in the range from about 1 to 4, a split Soret band is observed which is independent of counterion and tentatively assigned to a dimer species. As the pH is made lower than 1, the spectra evolve to reveal the presence of porphyrin aggregates. As in the case of the well-known aggregates of the related tetra(*p*-sulfonatophenyl)porphyrin (TSPP) diacid, the concentration of spectroscopically distinguishable aggregates increases with increasing ionic strength or decreasing pH. Unlike aggregates of TSPP, however, TCPP aggregates below pH 1 have visible absorption spectra which depend on the counterion, which is Cl^- or NO_3^- in this study. In this work, we present visible absorption, light-scattering, and resonance Raman spectra of TCPP diacid in its monomer, dimer, and aggregated forms and attempt to understand the structural basis for counterion-dependent structure and excitonic coupling in the aggregates. Evidence is presented for intercalation of inorganic counterions between porphyrin molecules in the aggregate, an effect which to our knowledge has not been previously reported.

1. Introduction

Dye aggregation and the resulting changes in visible light absorption have important consequences in nature and in technological applications. For example, porphyrin aggregates play specialized roles in photosynthetic plants and organisms,^{1,2} cyanine dye aggregates function as sensitizers in color photography,³ and self-assembled chromophore aggregates have potential uses as nonlinear optical materials.⁴ Transition moment coupling of strongly absorbing dyes can result in dramatic perturbations to the electronic spectra of dimers and higher aggregates.^{5–7} Especially interesting are strongly coupled aggregates with delocalized excitonic states, which may possess interesting optical properties such as superradiance.⁸ Conventional nomenclature distinguishes J (red-shifted)- and H (blue-shifted)-aggregate transitions in which the monomer transition dipoles are aligned parallel and perpendicular, respectively, to the line connecting neighboring molecules in the aggregates. J-aggregates of a wide variety of cyanine dyes have been studied,^{9–11}

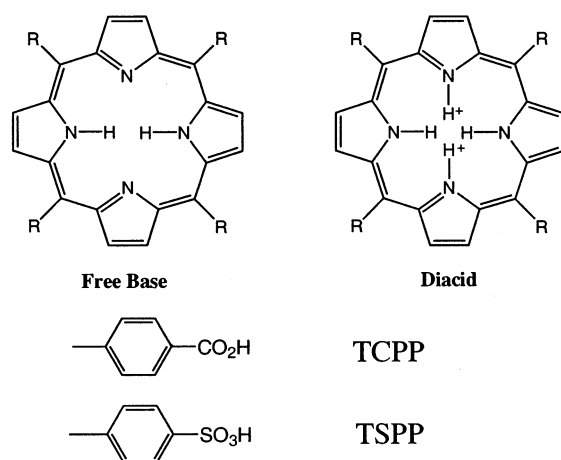
but among the porphyrins most of the attention has focused on tetra(*p*-sulfonatophenyl)porphyrin (TSPP) (Chart 1), where J-aggregates of the diacid form are observed in aqueous solution at low pH and high ionic strength.^{12–15}

The pK_a for the protonated diacid of TSPP is about 5.¹⁴ Below pH 5, TSPP exists as a zwitterionic species carrying negative charges at the peripheral SO_3^- groups and positive charges at the center of the porphyrin ring. In the diacid species (referred to here as $\text{H}_2\text{TSPP}^{2-}$, which assumes that all four sulfonate groups are ionized), the peripheral phenyl rings are rotated approximately 90° relative to their positions in the free base, making them nearly coplanar with the porphyrin ring and facilitating aggregation.¹⁶ The four N–H bonds at the center of the porphyrin ring have been reported to adopt a saddle structure in the diacid, facilitating hydrogen bonding with SO_3^- groups of neighboring porphyrins.¹⁷ Cartoons depicting the structure of the J-aggregate show the monomer units stacked as in a slipped deck of cards, with the negative charges on the periphery of one molecule overlapping the positive charges in the center of the neighboring porphyrin.^{14,18} Close association of the π orbitals of neighboring molecules leads to strong exciton

- (1) Hu, X.; Schulten, K. *Phys. Today* **1997**, 50, 28.
- (2) White, W. I. In *The Porphyrins*; Dolphin, D., Ed.; Academic: New York, 1979; Vol. V.
- (3) Gilman, P. B. In *Photographic Sensitivity*; Cox, R. J., Ed.; Academic Press: London, 1973.
- (4) Bohn, P. W. *Annu. Rev. Phys. Chem.* **1993**, 44, 37.
- (5) Knapp, E. W. *Chem. Phys.* **1984**, 85, 73.
- (6) Kasha, M.; Rawls, H. R.; El-Bayoumi, M. A. *Pure. Appl. Chem.* **1965**, 11, 371.
- (7) Rhodes, W. *J. Am. Chem. Soc.* **1961**, 83, 3609.
- (8) Scholes, G. D. *Chem. Phys.* **2002**, 275, 373 and other articles in this issue.
- (9) Spitz, C.; Knoester, J.; Ouart, A.; Daehne, S. *Chem. Phys.* **2002**, 275, 271.
- (10) Fidler, H.; Terpstra, J.; Wiersma, D. J. *Chem. Phys.* **1991**, 94, 6895.
- (11) Ohta, K.; Yang, M.; Fleming, G. R. *J. Chem. Phys.* **2001**, 115, 7609.

- (12) Kano, H.; Kobayashi, T. *J. Chem. Phys.* **2001**, 116, 184.
- (13) Ohno, O.; Kaizu, Y.; Kobayashi, H. *J. Chem. Phys.* **1993**, 99, 4128.
- (14) Maiti, N. C.; Ravikanth, M.; Mazumdar, S.; Periasamy, N. *J. Phys. Chem.* **1995**, 99, 17192.
- (15) Fleischer, E. B.; Palmer, J. M.; Srivastava, T. S.; Chatterjee, A. J. *J. Am. Chem. Soc.* **1972**, 94, 3162.
- (16) Stone, A.; Fleischer, E. B. *J. Am. Chem. Soc.* **1968**, 90, 2735.
- (17) Rubires, R.; Crusats, J.; El-Hachemi, Z.; Jaramillo, T.; López, M.; Valls, E.; Farrera, J.-A.; Ribó, J. M. *New J. Chem.* **1999**, 23, 189.
- (18) Akins, D. L.; Zhu, H.-R.; Guo, C. *J. Phys. Chem.* **1996**, 100, 5420.

Chart 1



coupling, and the resulting J-aggregate absorption is exchange narrowed.⁵ This narrow line width and the observation of strong resonance light scattering¹⁹ imply the Soret band excitation is delocalized over a number of porphyrin molecules. The coherence length, that is, the number of molecules sharing the exciton, has been reported to be approximately 7,¹² although the physical size of the aggregate is much larger.^{14,20} One interesting property of H₂TSPP²⁻ aggregates is that they exhibit flow-induced linear dichroism¹² and swirling-induced circular dichroism.²¹ Resonance Raman spectra of aggregated H₂TSPP²⁻ have been reported by Akins et al.²² and Chen et al.²³

In this work, we report evidence for aggregation of the water-soluble porphyrin tetra(*p*-carboxyphenyl)porphyrin (TCPP, Chart 1) in acid solution, and we report the resulting excitonic spectra which depend on the counteranion. Protonation of the pyrrole nitrogens has been reported to occur at a pH of about 5, and the pK_a of the carboxylic acid functions is also approximately 5.²⁴ Thus, below pH 5, TCPP is a doubly charged diacid H₂TCPP²⁺. Pasternack et al.²⁴ previously observed dimerization of the free base TCPP at pH 7.5, as evidenced by deviations from Beer's law and subtle changes in the appearance of the Soret band. Recently, complexes of TCPP with viologens and formation of dimers of TCPP in neutral solution were reported.²⁵ On the other hand, only a few reports of extended aggregates of TCPP have appeared in the literature. Akins et al.¹⁸ obtained the resonance Raman spectrum of H₂TCPP²⁺ aggregates in aqueous trifluoroacetic acid solution. Grätzel et al.²⁶ observed spectroscopic signatures of aggregation in ZnTCPP in acid solution. A two-dimensional hydrogen-bonded network of TCPP on graphite has been reported.²⁷ The limited number of previous studies of aqueous aggregates of TCPP may be a consequence

of its low solubility in acid solution, a problem which was circumvented in this work by using poly(vinyl alcohol) (PVA) to slow precipitation of TCPP aggregates (see, for example, ref 26). We compare the electronic absorption, light-scattering, NMR, and resonance Raman spectra of aggregates of the diacid, H₂TCPP²⁺, in aqueous HCl and HNO₃ solution, at a pH slightly less than 1, and also examine the spectra of the counterion-independent form that is observed above pH 1. The counterion dependence of the excitonic spectra of these aggregates opens up the possibility to tune the electronic properties and to further explore the correlations of structural and electronic properties in these kinds of self-assembled systems.

2. Experimental Section

TCPP and TSPP (as the dihydrochloride salt) were obtained from Porphyrin Products, Inc. (Logan, UT) and used as received. Poly(vinyl alcohol) (PVA) (average molecular weight of 30 000–70 000) was obtained from Sigma Chemical Co. and was used to prevent precipitation of TCPP aggregates at low pH. It was verified that similar spectra are obtained, shortly after sample preparation, in the absence of PVA. Precipitated samples of TCPP aggregates revealed a glassy blue-green phase (for which no crystals could be obtained for X-ray measurements) and ordered crystals of salt. Aqueous solutions were prepared in Millipore deionized water and were buffered using either KCl and HCl or KNO₃ and HNO₃. Solutions with a nominal pH of 0.9 contained either 0.27 M HCl and 0.10 M KCl, or 0.5 M HNO₃ and 0.25 M KNO₃. Solutions at pH 1 and higher were prepared according to procedures in ref 28. In the absence of PVA, TCPP has very low solubility in water below pH 5; therefore, samples were initially prepared in 0.01 M NaOH, then acidified and combined with saturated PVA solution to bring the final PVA concentration to 1.4 g/100 mL. Absorption spectra were measured in 1 cm quartz cells with 0.5 nm resolution at room temperature using a Shimadzu UV-2501 spectrometer. The concentration of TCPP and TSPP used in absorption and light-scattering spectroscopy was 5.0 × 10⁻⁶ M. Resonance Raman spectra of solutions containing 5.0 × 10⁻⁵ M porphyrin were excited using the 457.9 nm line of a Coherent Innova 400 Argon ion laser, with 100 mW of power at the sample and 90° scattering geometry. Solutions for Raman measurements included 0.5 M NO₃⁻ ion as an internal intensity standard, and samples were circulated through a glass capillary cell. The scattered light was analyzed using a double monochromator and photomultiplier tube detection. Fluorescence (emission) spectra were collected on the same instrumentation used to obtain Raman spectra. The stability of each sample was verified by measuring the absorption spectrum before and after gathering the Raman and fluorescence spectra. Resonance light-scattering (RLS) and fluorescence excitation spectra were measured on a Hitachi F-4500 fluorescence spectrophotometer with a 150 W xenon lamp, using right angle geometry and synchronous scanning mode. Samples for RLS experiments were contained in poly-(methyl methacrylate) cuvettes. The background light scattering (less than 100 counts per second) of a solution containing only PVA was subtracted from the light-scattering spectra of the aggregated samples. ¹H NMR spectra of 5 × 10⁻⁴ M samples of porphyrin were measured in D₂O and in ethanol-*d*₆ on a 500 MHz Bruker instrument.

3. Results

3.1. Electronic Absorption Spectra. Figure 1 compares the visible absorption bands of TCPP in basic solution, in ethanol containing approximately 0.3 M HNO₃, and in aqueous HNO₃ at pH 0.9. The strong band at about 300 nm is from NO₃⁻. In water at a pH above 5, the carboxylic acid groups of TCPP are ionized, and the Soret band maximum appears at 414 nm. The

- (19) (a) Pasternack, R. F.; Collings, P. J. *Science* **1995**, 269, 935. (b) Collings, P. J.; Gibbs, E. J.; Starr, T. E.; Vafek, O.; Yee, C.; Pomerance, L. A.; Pasternack, R. F. *J. Phys. Chem. B* **1999**, 103, 8474.
- (20) Micali, N.; Mallamace, F.; Romeo, A.; Purello, R.; Scolaro, L. M. *J. Phys. Chem. B* **2000**, 104, 5897.
- (21) Ribó, J. M.; Crusats, J.; Sagués, F.; Claret, J.; Rubires, R. *Science* **2001**, 292, 2063.
- (22) Akins, D. L.; Zhu, H.-R.; Guo, C. J. *J. Phys. Chem.* **1994**, 98, 3618.
- (23) Chen, D.-M.; He, T.; Cong, D.-F.; Zhang, Y.-H.; Liu, F.-C. *J. Phys. Chem. A* **2001**, 105, 3981.
- (24) Pasternack, R. F.; Huber, P. R.; Boyd, P.; Engasser, G.; Francesconi, I.; Gibbs, E.; Fosella, P.; Cerio Ventura, G.; Hinds, L. de C. *J. Am. Chem. Soc.* **1972**, 94, 4511.
- (25) Clarke, S. E.; Wamser, C. C.; Bell, H. E. *J. Phys. Chem.* **2002**, 106, 3235.
- (26) Kalyanasundara, K.; Vlachopoulos, V.; Krishnan, K.; Minner, A.; Grätzel, M. *J. Phys. Chem.* **1987**, 91, 2342.
- (27) Lei, S. B.; Wang, C.; Yin, S. X.; Wang, H. N.; Xi, F.; Liu, H. W.; Xu, B.; Wan, L. J.; Bai, C. L. *J. Phys. Chem. B* **2001**, 105, 10838.

- (28) *CRC Handbook of Chemistry and Physics*, 75th ed.; Lide, D. R., Ed.; CRC Press: Boca Raton, FL, 1995.

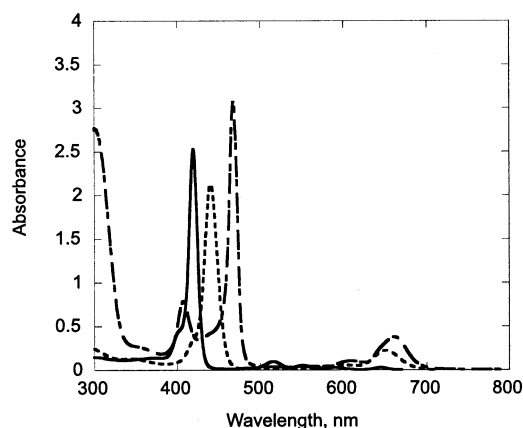


Figure 1. Absorption spectrum of TCPP free base in water at pH 10 (full line), of $\text{H}_2\text{TCPP}^{2+}$ in acidified ethanol (dashed line), and of $\text{H}_2\text{TCPP}^{2+}$ aggregates in aqueous HNO_3 at pH 0.9 (dot-dashed line). The porphyrin concentration in each case is 5×10^{-6} M.

Table 1. Absorption Maxima λ_{max} of the Soret and Q-Bands of TCPP

porphyrin	solvent	λ_{max} , nm	
		Soret band	Q-band
TCPP	water, pH 10	414	516, 552, 591, 645
TCPP	ethanol	416	513, 545, 588, 644
$\text{H}_2\text{TCPP}^{2+}$	ethanol/0.3 M H^+	440	599, 651
$\text{H}_2\text{TCPP}^{2+}$	water, pH 1.2	404, 444	520, 555, 592, 648
$\text{H}_2\text{TCPP}^{2+}$	water/ HNO_3 , pH 0.9	406, 467	610, 662
$\text{H}_2\text{TCPP}^{2+}$	water/HCl, pH 0.9	417	664

Q-bands for the ionized free base display the 0–0 and 0–1 vibronic components of the nondegenerate Q_x and Q_y bands (etio pattern), as expected for D_{2h} symmetry, as shown in Table 1. In ethanol/ HNO_3 , the carboxyl groups and the porphyrin nitrogens are all protonated to form $\text{H}_2\text{TCPP}^{2+}$, and the x , y components of the Q-band collapse as expected for four-fold symmetry. An identical spectrum was obtained in 0.3 M HCl/ethanol solution. Because evidence has been presented that porphyrin aggregation is inhibited in alcohol solution,²⁹ we consider the peak at 440 nm in ethanol/ HNO_3 to represent the $\text{H}_2\text{TCPP}^{2+}$ monomer. Light-scattering measurements presented below also support this conclusion. In aqueous HNO_3 at pH < 1, on the other hand, the Soret band has both blue-shifted (406 nm) and red-shifted (467 nm) components, the latter being more intense and somewhat sharper than the Soret band of the monomer diacid in ethanol. Because there are only minor shifts in the Soret and Q-bands of TCPP free base between ethanol and water (see Table 1), the large difference in the absorption spectrum of the diacid in ethanol and water is attributed here to aggregation. We tentatively assign the red- and blue-shifted Soret band components of $\text{H}_2\text{TCPP}^{2+}$ in aqueous nitric acid at pH < 1 to J- and H-aggregate transitions, respectively. The spectrum of $\text{H}_2\text{TCPP}^{2+}$ in aqueous HNO_3 is qualitatively similar to that observed by Akins et al.¹⁸ for TCPP in aqueous trifluoroacetic acid, where the putative H- and J-bands appear at 414 and 469 nm.

Figure 2 compares the absorption spectrum of TCPP obtained in aqueous HNO_3 at pH 0.9 to that in aqueous HCl at the same pH. In the latter, there is only a single blue-shifted Soret band. As compared to the half-width (fwhm) of the Soret band in

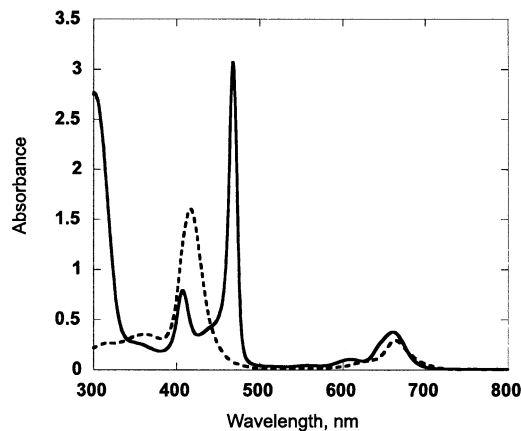


Figure 2. Comparison of absorption spectra of $\text{H}_2\text{TCPP}^{2+}$ aggregates in aqueous HCl (dashed line) and HNO_3 (full line), both at pH 0.9.

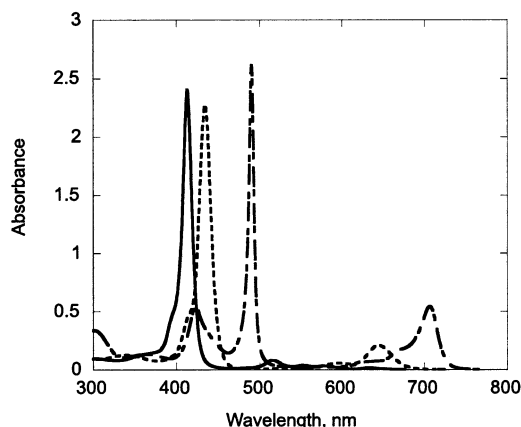


Figure 3. Absorption spectrum of TSPP free base (full line), of $\text{H}_2\text{TSPP}^{2-}$ in water at pH 4 (dashed line), and of aggregated $\text{H}_2\text{TSPP}^{2-}$ in aqueous HNO_3 at pH 0.8 (dot-dashed line).

$\text{H}_2\text{TCPP}^{2+}$ in acidified ethanol ($\Delta\tilde{\nu}_{1/2} = 980 \text{ cm}^{-1}$), that for the Soret band in HCl solution is broader by almost a factor of 2 ($\Delta\tilde{\nu}_{1/2} = 1840 \text{ cm}^{-1}$), while the red-shifted (J-band) peak in HNO_3 solution is narrower ($\Delta\tilde{\nu}_{1/2} = 521 \text{ cm}^{-1}$) than the monomer absorption band. The spectra in Figure 2 can be compared to the spectra of monomeric and aggregated forms of TSPP shown in Figure 3. In basic solution, TSPP exists as a monomer anion with a charge of -4 from the sulfonato groups, and the Soret band appears at 413 nm. At pH 4, the diacid species forms, and the Soret band red-shifts to 434 nm. At still lower pH, the characteristic spectrum of aggregated $\text{H}_2\text{TSPP}^{2-}$ is observed, showing the narrow J-band at about 490 nm and a weaker H-band at 421 nm. The spectra at low pH of TCPP in nitric acid solution and TSPP have similar features, including broad Q-bands which are red-shifted as compared to those of the monomer. The slight difference in the absorption maxima for monomer forms of TSPP versus TCPP (free base and diacid) reveals that there is little electronic interaction between the acid functional groups and the π electron system of the porphyrin. The appearance of the spectrum of aggregated $\text{H}_2\text{TSPP}^{2-}$ has been reported not to depend on the nature of the positively charged inorganic counterions,³¹ although the intensity of the aggregate transition does increase with increasing ionic strength.

(30) (a) Miller, G. A. *J. Phys. Chem.* **1978**, 82, 616. (b) Stanton, S. G.; Pecora, R. J. *J. Chem. Phys.* **1981**, 75, 5615.

(31) Maiti, N. C.; Mazumdar, S.; Periasamy, N. *J. Phys. Chem. B* **1998**, 102, 1528.

(29) Gallagher, W. A.; Elliot, W. B. *Ann. N.Y. Acad. Sci.* **1973**, 206, 463.

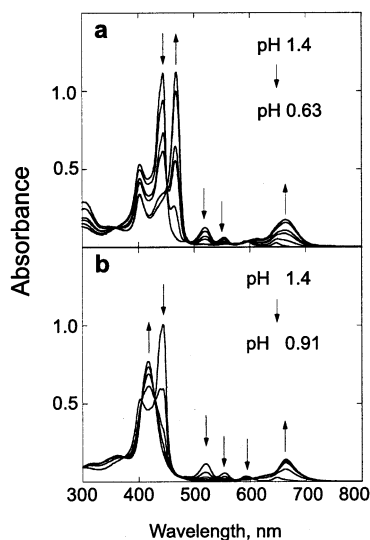


Figure 4. Absorption spectra of H_2TCPP^{2+} (a) in aqueous HNO_3 and (b) in aqueous HCl, as a function of pH.

As demonstrated in Figure 2, however, the spectrum of aggregated H_2TCPP^{2+} depends on the nature of the counteranion. We also obtained spectra of TCPP in aqueous HBr at a similar pH (not shown) and observed strongly overlapped bands at 439 and 469 nm, while in acetic acid the Soret band was found to be similar to that for H_2TCPP^{2+} in ethanol. Evidently, the nature of the counterion influences the tendency of H_2TCPP^{2+} to aggregate as well as the resulting structure of the aggregate.

Figure 4 shows how the Soret band of H_2TCPP^{2+} evolves as the pH is lowered in aqueous HNO_3 and HCl solutions. At a pH above 1 and below 4.5, in either solution, the Soret band of H_2TCPP^{2+} is split into two components at about 444 (with a shoulder at 439) and 404 nm. Note also the unexpected structure in the Q-band region, which suggests that the symmetry is less than four-fold. The appearance of the spectrum above pH 1 was found not to depend on the nature of the acid. However, as the pH is lowered, different spectra are obtained in the presence of HNO_3 and HCl. We tentatively assign the spectrum observed above pH 1 to a dimer of H_2TCPP^{2+} . We propose that in lower pH solutions containing Cl^- or NO_3^- , counterion-dependent aggregates are formed.

The pH-dependent spectra in Figure 4a and b exhibit apparent isosbestic points at about 450 and 428 nm, respectively, as well as blurred crossing points in the Q-band regions. On closer examination, the spectra shown in Figure 4 do not cross at a single wavelength. This is in contrast to the results observed when the spectrum of TSPP is measured in a similar pH range, where a fairly sharp isosbestic point is observed at 453 ± 0.5 nm (this work, see also ref 23). This suggests that there are more than two forms of TCPP which contribute to the spectra of Figure 4. In TCPP in either nitric or hydrochloric acid solution, there is a blue-shifted Soret band at about 400 nm, which remains distinct as the pH is lowered in nitric acid solution but appears to be lost or to merge with the presumed aggregate transition at 417 nm in aqueous HCl.

Figure 5 illustrates the influence of added electrolyte on the spectra of TCPP diacid. In HNO_3 solution, the putative J-band at 467 nm increases as the KNO_3 concentration is increased (Figure 5a), and in HCl solution the feature at 417 nm increases

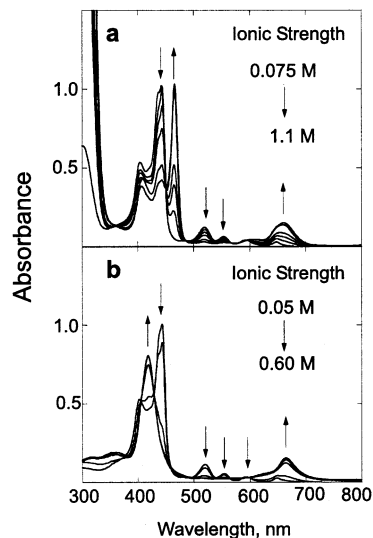


Figure 5. Absorption spectra of H_2TCPP^{2+} (a) in aqueous HNO_3 and (b) in aqueous HCl, as a function of ionic strength, adjusted by the addition of KNO_3 or KCl, respectively.

in intensity as KCl is added. These results are similar to those for other water-soluble porphyrins,² where increasing ionic strength has been shown to favor aggregate formation. Similar experiments employing mixed ethanol/water solutions containing TCPP and either nitric or hydrochloric acid (see figure in the table of contents) also reveal increasing intensity of the aggregate transitions as the ratio of water to ethanol increases. These results are indicative of hydrophobic interactions which drive the aggregation process. The counterion-dependent aggregates appear to be kinetically fairly stable. For example, addition of KCl to the aggregated form in HNO_3 does not change the absorption spectrum, nor does addition of KNO_3 to the HCl aggregate perturb the spectrum, at least over the course of several hours. If, however, the salt is added to a freshly prepared solution of the aggregate, or if a monomer solution is aggregated by the simultaneous addition of HNO_3 and KCl, or by the addition of HCl and KNO_3 , very broad absorption spectra are observed, which suggest that a mixture of aggregated species is obtained.

3.2. Resonance Light Scattering. As has been shown by Pasternack and co-workers, resonance light scattering (RLS) is a powerful tool for detecting the presence of electronically coupled porphyrin aggregates.¹⁹ Light-scattering spectra were measured in this work using a conventional fluorescence spectrometer in synchronous scan mode, that is, by scanning equal excitation and emission wavelengths to generate an excitation profile for the elastically scattered light. Although any chromophore can exhibit RLS when excited within its absorption band,³⁰ in the absence of aggregation the effect is generally offset by absorption. Figure 6a–e displays light-scattering and absorption spectra for various forms of TCPP, all in solutions containing 5.0×10^{-6} M TCPP. For comparison, similar data are shown in Figure 6f for 5.0×10^{-6} M H_2TSPP^{2-} in a solution (pH 1.8) containing only a small absorption band from the J-aggregate. A strong and sharply peaked RLS signal is observed just to the red of the H_2TSPP^{2-} J-aggregate absorption. This strong signal, as has been previously reported,¹⁹ is the result of a delocalized excitonic state in which the chromophores are strongly coupled electronically. Figure 6a and

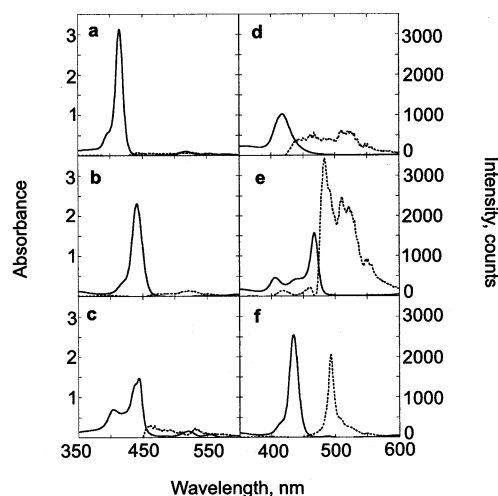


Figure 6. Absorption (solid lines) and resonance light-scattering (dashed lines) spectra of (a) TCPP free base in water, (b) H₂TCPP²⁺ in acidified ethanol, (c) H₂TCPP²⁺ in water at pH 1.2, (d) H₂TCPP²⁺ in aqueous HCl at pH 0.9, (e) H₂TCPP²⁺ in aqueous HNO₃ at pH 0.9, and (f) H₂TSPP²⁻ in aqueous HNO₃ at pH 1.8.

b shows absorption and light-scattering data for TCPP in water at pH 10 and in ethanol/HNO₃. The low signal obtained in these samples, $\lesssim 100$ counts/s, is evidence that these solutions contain monomer forms of TCPP. Figure 6c shows absorption and light-scattering data for H₂TCPP²⁺ in water at pH 1.2. Again, little light-scattering signal is obtained, consistent with the existence of a dimer or other small aggregate at this pH. The slight increase in the light-scattering signal in this sample, as compared to that from the monomer forms in Figure 6a and b, may be due to a small amount of aggregate that has begun to form at this pH. Figure 6d and e shows the absorption and light-scattering data for H₂TCPP²⁺ in aqueous hydrochloric acid and nitric acid, respectively, at pH ≈ 0.9 . In HCl solution, there is weak (~ 500 counts/s) light scattering over a broad range of wavelengths to the red of the absorption band. This is most likely nonresonance light scattering resulting from a distribution of aggregate sizes. The absence of a sharp and strong RLS peak, in agreement with the lack of exchange narrowing of the Soret band, implies that the aggregates which form in HCl solution are not strongly coupled electronically. In the case of H₂TCPP²⁺ in nitric acid (Figure 6e), however, a much stronger light-scattering signal is obtained (>3000 counts/s), having a fairly sharp peak slightly to the red of the J-aggregate absorption maximum superimposed on a broad background. We propose that the sharp light-scattering signal is resonance light scattering associated with the J-aggregate transition and that it is superimposed on a broad nonresonance light-scattering signal resulting from a distribution of physical aggregate sizes in which the electronic coupling is relatively weak as compared to that in the J-aggregate of TSPP. As discussed below, the J-aggregate absorption of H₂TCPP²⁺ at 467 nm (nitric acid) is about one-half as broad as the monomer absorption band in acidic ethanol, indicating that the exciton state is delocalized over about four molecules. For the J-aggregate of H₂TSPP²⁻, on the other hand, comparison of the monomer and aggregate absorption widths suggests that the coherence number is approximately eight molecules. This comparison is in accord with the much stronger RLS signal in TSPP J-aggregates as compared to TCPP

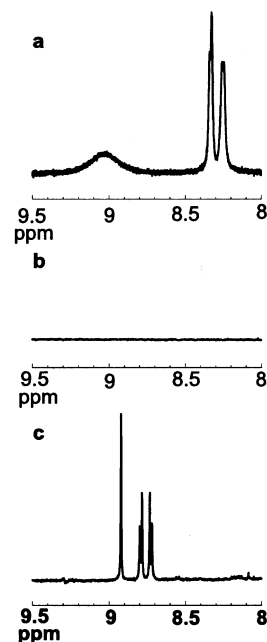


Figure 7. ¹H NMR spectrum of (a) free base TCPP in D₂O at pH 10, (b) H₂TCPP²⁺ in aqueous HNO₃ at pH 0.9, and (c) H₂TCPP²⁺ in acidified ethanol-d₆.

J-aggregates, because the RLS signal increases with increasing excited-state delocalization.

3.3. NMR Spectra. Figure 7a–c shows the ¹H NMR spectra of TCPP monomer in basic D₂O, H₂TCPP²⁺ in D₂O/HNO₃ at pH 0.9, and H₂TCPP²⁺ in HNO₃/ethanol-d₆, respectively. The monomer free base (Figure 7a) shows a broad peak at about 9.1 ppm assigned to the β pyrrole hydrogens and two peaks between 8.2 and 8.4 ppm assigned to the phenyl protons. In the diacid in ethanol (Figure 7c), the pyrrole protons display a sharp peak at about 8.9 ppm, and the phenyl protons are observed as a pair of doublets shifted downfield from their positions in the free base. These assignments are similar to those reported for TSPP monomer free base and diacid.³¹ In aqueous acid solution, as shown in Figure 7b for TCPP in nitric acid, there is no observable NMR signal. We also failed to obtain NMR spectra for samples in HCl at pH 0.9, and in either acid at pH 1.2, where the dimer is assumed to prevail. It was, however, difficult to confirm the existence of only dimers in the pH 1.2 solution, because the concentrations required for NMR analysis resulted in absorbances too high to be measured even in short path length cells. The existence of the dimer was inferred from the dark yellow color of the solution and the measured pH, but the possibility that higher aggregates were present in the NMR “dimer” sample cannot be ruled out. NMR studies of water-soluble porphyrin dimers have been previously reported,³² however, such studies on H₂TSPP²⁻ have noted the loss of NMR signal in aggregated samples and attributed it to inhomogeneous broadening.^{14,17} The loss of signal for H₂TCPP²⁺ in aqueous acid solutions reveals that a range of proton environments is possible in the aggregated species, and possibly also in the dimer. Alternatively, a fast exchange between different forms could lead to broadening and loss of signal.

3.4. Resonance Raman Spectra. Figure 8 shows resonance Raman (RR) spectra of the free base TCPP in basic solution,

(32) Kano, K.; Takei, M.; Hashimoto, S. *J. Phys. Chem.* **1990**, *94*, 2181.

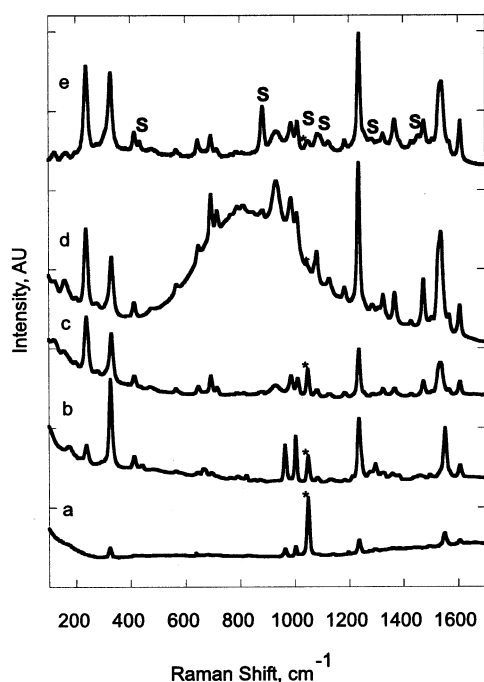


Figure 8. Resonance Raman spectra of 5.0×10^{-5} M solutions, excited at 457.9 nm, of (a) TCPP free base monomer in water at pH 10, (b) $\text{H}_2\text{TCPP}^{2+}$ in water at pH 1.2, (c) $\text{H}_2\text{TCPP}^{2+}$ in aqueous HCl at pH 0.9, (d) $\text{H}_2\text{TCPP}^{2+}$ in aqueous HNO_3 at pH 0.9, and (e) $\text{H}_2\text{TCPP}^{2+}$ in acidified ethanol. The asterisk marks the NO_3^- band at 1048 cm^{-1} , used as an internal standard. In (e), the solvent Raman bands are marked with "S", and the background due to fluorescence has been subtracted.

the dimer of $\text{H}_2\text{TCPP}^{2+}$ at pH 1.2, aggregated $\text{H}_2\text{TCPP}^{2+}$ in aqueous acid (nitric and hydrochloric) at pH 0.9, and the diacid monomer in ethanol, all excited at 457.9 nm. This wavelength is somewhat to the red of the Soret band in all but the nitric acid solution, in which case the excitation is within the J-band. The peak frequencies and relative Raman intensities in these samples are detailed in Table 2. All solutions contained equal concentrations of nitrate ion so that the 1048 cm^{-1} Raman band of NO_3^- could be used as an intensity standard. In ethanol solution, the concentration of free NO_3^- (versus HNO_3) is uncertain, and the 1048 cm^{-1} is strongly overlapped by solvent transitions; hence, the reported intensities in ethanol solution cannot be meaningfully compared to those of other samples, but may be used to compare relative intensities of the various Raman bands in ethanol solution. In this section, we discuss the observed Raman bands using assignments gleaned from a number of references, including RR studies of TSPP monomer and aggregates reported by Chen et al.,²³ and by Akins and co-workers,²² and the thorough assignments of nickel tetraphenylporphyrin reported in ref 33.

It is clear from Table 2 that the Raman shifts of the putative dimer are very similar to those of the free base TCPP, although the former are generally more intense due to stronger resonance enhancement at the excitation wavelength used. On the other hand, the peak frequencies in the aggregated samples resemble those of the $\text{H}_2\text{TCPP}^{2+}$ monomer in ethanol, consistent with the noncovalent nature of the intermolecular interactions in aggregates built up from diacid monomers. The resemblance of the dimer Raman spectrum to that of the free base monomer

Table 2. Raman Shifts $\Delta\tilde{\nu}$ in cm^{-1} and Intensities Relative to the Nitrate Band at 1048 cm^{-1} (See Text) for (a) Free Base TCPP Monomer, (b) the $\text{H}_2\text{TCPP}^{2+}$ Dimer at pH 1.2, Aggregated $\text{H}_2\text{TCPP}^{2+}$ in (c) HCl and (d) HNO_3 at pH 0.9, and (e) $\text{H}_2\text{TCPP}^{2+}$ in Ethanol

(a) monomer		(b) dimer		(c) HCl-agg.		(d) HNO_3 -agg.		(e) diacid	
$\Delta\tilde{\nu}$	int.	$\Delta\tilde{\nu}$	int.	$\Delta\tilde{\nu}$	int.	$\Delta\tilde{\nu}$	int.	$\Delta\tilde{\nu}$	int.
325	0.16	238	0.62	239	1.9	238	8.9	239	5.4
		327	3.3	330	1.7	330	6.6	329	4.8
		413	0.47	413	0.36	413	1.7	415	1.1
		566	0.09	566	0.17	566	1.0	567	0.36
		645	0.13	647	0.25	647	1.5	647	0.88
		667	0.30						
		695	0.18	693	0.63	693	5.3	693	1.1
				715	0.24	715	2.6	715	.48
		763	0.09						
		791	0.15						
		823	0.20						
		872	0.09	881	0.11	883	0.9	883	2.9
				931	0.36	931	6.0	933	0.89
967	0.13	964	1.4						
1003	0.15			986	0.10	986	6.1	986	1.2
		1003	1.7	1010	0.65	1010	5.1	1010	1.8
1048	1.0	1048	1.0	1048	1.0	1048	1.0	1048	1.0
		1082	0.18	1081	0.24	1081	3.4	1085	0.79
		1130	0.12	1127	0.13	1127	1.8	1125	0.59
		1183	0.08	1183	0.17	1184	1.6	1184	0.65
		1236	0.23	1235	1.7	1235	17	1237	7.4
		1296	0.63						
				1324	0.27	1324	2.5	1325	0.62
				1368	0.29	1368	3.4	1368	1.8
				1474	0.55	1474	5.4	1475	1.5
				1536	1.2	1536	12	1538	4.3
1550	0.22	1552	1.9						
1606	0.07	1607	0.47	1607	0.51	1607	3.5	1607	2.5

is at first surprising, because at pH 1.2 the diacid species is expected. However, both the free base and the dimer absorption spectra reveal *x* and *y* components of the Q-bands, evidence that the symmetry is D_{2h} rather than D_{4h} . Consistent with this, we observed depolarization ratios close to 1/3 in the RR spectrum of the dimer and free base, evidence of resonance with a nondegenerate excited state. These results support a model for the dimer structure in which there are strong perturbations to the porphyrin core.

A few modes are shifted in the diacid and the aggregates relative to the free base and the dimer. There is an apparent red-shift of the ν_2 band from about 1550 cm^{-1} in the monomer free base and dimer spectra to about 1536 cm^{-1} in the spectra of the diacid and aggregates. This band is assigned to the stretches of the $\text{C}_\alpha\text{--C}_m$ and $\text{C}_\beta\text{--C}_\beta$ bonds in ref 23; however, Akins et al.²² attribute the 1536 and 1550 cm^{-1} bands to different vibrational modes. A band observed at 967 cm^{-1} in the monomer free base and dimer spectra, assigned to $\nu(\text{C}_\alpha\text{--C}_m)$ in ref 22, disappears in the spectra of the diacid and aggregates, which in turn display two new bands at 931 and 986 cm^{-1} . In J-aggregates of TSPP, a band at 986 cm^{-1} was reported and attributed to $\nu(\text{C}_\alpha\text{--C}_m)$, blue-shifted from its frequency in the monomer free base.²² The assignment of the broad band at 931 cm^{-1} is uncertain; however, we note that a similar feature is apparent in the Raman spectra of aggregated TCPP in aqueous trifluoroacetic acid reported in ref 18.

Although the peak frequencies of various forms of TCPP are similar, there are dramatic differences in resonance Raman intensity, in part because the Soret band positions are different and we are comparing spectra excited at the same excitation wavelength. Overall, Raman intensities are largest in the HNO_3

(33) Li, X.-Y.; Czernuszewicz, R. S.; Kincaid, J. R.; Su, Y. O.; Spiro, T. G. *J. Phys. Chem.* **1990**, *94*, 31.

aggregate because the excitation is most favorable to resonance enhancement in this case. However, there are considerable differences in the relative Raman intensities in the different samples. On going from monomer free base to monomer diacid, there is a strong increase in the intensities of two low frequency modes at approximately 238 and 330 cm^{-1} , which have been variously assigned to out-of-plane motion of the pyrrolic nitrogens, that is, ruffling and doming motions, respectively.⁴⁵ There is a large increase in the intensity of both of these modes, particularly the one at 330 cm^{-1} , on going from the monomer free base to the dimer. The enhancement of low-frequency modes in aggregates has been previously reported and will be discussed further in section 4.4. Here we note that even in the absence of aggregation ($\text{H}_2\text{TCCPP}^{2+}$ in ethanol), there is considerable enhancement of the low-frequency bands relative to, for example, the intensity of the totally symmetric vibration at 1237 cm^{-1} , assigned to $\nu_1(\text{C}_m-\phi)$. In the free base monomer, the doming mode is about $2/3$ as strong as ν_1 (the strongest peak), and the ruffling mode is below our detection limit. In the diacid monomer, the doming mode is also about $2/3$ as strong as ν_1 , but the ruffling mode is even stronger. In the diacid monomer and HCl aggregate, the ruffling mode is stronger than the doming mode by about 10%, while in the HNO_3 aggregate, the ruffling mode is 30% more intense than doming. It is clear that, in addition to the increase in intensity of the low-frequency modes upon protonation of the pyrrolic nitrogens, there are further perturbations to their intensity associated with aggregation.

The absorption maximum of the aggregate in HCl is similar to that of the monomer free base, albeit broader. It is therefore possible to qualitatively compare the absolute intensities in these two samples and realize that there is a clear enhancement of the resonance Raman signal in the aggregate. For example, the Raman band at 330 cm^{-1} in the aggregate in HCl is more than 10 times larger than that in the monomer, while the bands at 1235 and 1607 cm^{-1} are enhanced by a factor of about 7. Akins has presented a theory of aggregation enhanced Raman scattering (AERS) in which the Raman signal is predicted to be enhanced by a factor equal to the number of molecules in the aggregate.^{34,35} Further studies of this enhancement will require resonance Raman data as a function of excitation wavelength.

The broad background which peaks at about 825 cm^{-1} in the resonance Raman spectrum of the aggregate in HNO_3 (Figure 8d) is reproducible and assigned to J-band fluorescence. It is not observed when longer wavelength excitation (488 nm) is used to measure the Raman spectrum. The Stokes shift $\tilde{\nu}_{\text{abs}} - \tilde{\nu}_{\text{fluor}}$ is only 400 cm^{-1} , consistent with the narrow line width

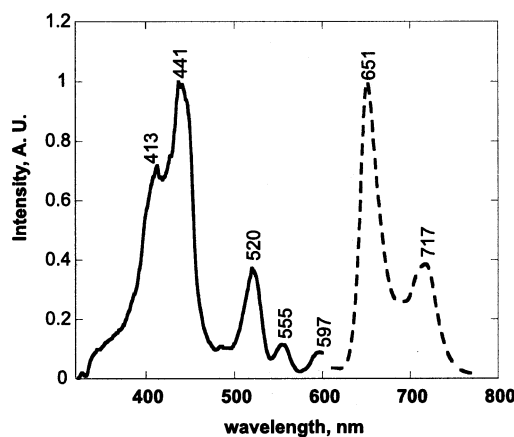


Figure 9. Fluorescence excitation (full line) and emission (dashed line) spectra of $\text{H}_2\text{TCCPP}^{2+}$ dimer at pH 1.2, $1 \times 10^{-6}\text{ M}$. The excitation spectrum was detected at 650 nm , and the emission spectrum was excited at 458 nm .

of the J-band absorption and emission features. Soret band fluorescence is fairly unusual, but near-resonance fluorescence in the case of J-aggregates is well known. Kano et al.³⁶ reported sharp fluorescence from the J-aggregates of $\text{H}_2\text{TSP}^{2+}$ with a vanishing Stokes shift and a lifetime of less than 0.5 ps . Apparently, the monomers in the J-aggregates of $\text{H}_2\text{TCCPP}^{2+}$ in HNO_3 solution are somewhat less strongly coupled, permitting a modest Stokes shift to be observed.

We also observed fluorescence in the Q-band regions in aggregated samples, but the emission (681 nm) is identical to that of the diacid monomer but less intense by several orders of magnitude. Furthermore, the excitation spectrum for this emission peaks at 440 nm , the absorption maximum of monomer diacid. This suggests that in the aggregates the Q-band fluorescence is quenched and the weak fluorescence observed is from residual monomer diacid. The fluorescence excitation and emission spectra of the dimer (pH 1.2), shown in Figure 9, are more interesting. There are two peaks in the excitation spectrum at 413 and 441 nm , similar to the wavelengths of the absorption maxima at 404 and 440 nm . The same emission spectrum is obtained when the fluorescence is excited at these two wavelengths. There are also maxima at the Q-band absorptions, although instrumental limitations prevented the excitation spectrum from being determined at wavelengths greater than 600 nm . The emission peak at 651 nm coincides with the longest wavelength peak (648 nm) in the absorption spectrum and thus is assigned to the 0–0 component of Q_x . Furthermore, the separation of the two peaks in the emission spectrum, 1420 cm^{-1} , is similar to the 1460 cm^{-1} separation of the 0–0 and 0–1 components of Q_x in the absorption spectrum. Finally, there is no emission maximum at 681 nm , where the fluorescence of $\text{H}_2\text{TCCPP}^{2+}$ monomer peaks. Thus, the absorption maximum at 440 nm at this pH does not appear to result from residual diacid monomer in equilibrium with some other species. These considerations lead us to conclude that the absorption spectrum of $\text{H}_2\text{TCCPP}^{2+}$ at pH 1.2 results from a single species with less than four-fold symmetry, rather than from a superposition of spectra of two forms of porphyrin.

4. Discussion

4.1. Effect of Counterions. We have shown that the visible absorption spectrum of $\text{H}_2\text{TCCPP}^{2+}$ in aqueous acidic solution at pH < 1 depends on the nature of the counterion. The influence

(34) Akins, D. L. *J. Phys. Chem.* **1986**, *90*, 1530.

(35) Akins, D. L.; Ozcelik, S.; Zhu, H.-R.; Guo, C. *J. Phys. Chem.* **1997**, *101*, 3251.

(36) Kano, H.; Kobayashi, T. *J. Chem. Phys.* **2002**, *116*, 184.

(37) Davis, R. C.; Ditson, S. L.; Fentiman, A. F.; Pearlstein, R. M. *J. Am. Chem. Soc.* **1981**, *103*, 6823.

(38) Osuka, A.; Maruyama, K. *J. Am. Chem. Soc.* **1988**, *110*, 4454.

(39) Kalyanasundaram, K. *Photochemistry of Polypyridine and Porphyrin Complexes*; Academic Press: London, 1992; Chapters 12 and 13.

(40) Gouterman, M. *J. Chem. Phys.* **1959**, *30*, 1139.

(41) Sundström, V.; Gillbro, T.; Gadonas, R. A.; Piskarskas, A. *J. Chem. Phys.* **1988**, *89*, 2754.

(42) (a) Wang, M.; Silva, G. L.; Armitage, B. A. *J. Am. Chem. Soc.* **2000**, *122*, 9977. (b) Chowdury, A.; Wachsmann-Hogiu, S.; Bangal, P. R.; Raheem, I.; Peteanu, L. A. *J. Phys. Chem. B* **2001**, *105*, 12196.

(43) Higgins, D. A.; Karimo, J.; Van den Bout, D. A.; Barbara, P. F. *J. Am. Chem. Soc.* **1996**, *118*, 4049.

(44) Webb, M. A.; Choi, M. Y.; Knorr, F. J.; McHale, J. L., to be submitted.

(45) Kano, H.; Saito, T.; Kobayashi, T. *J. Phys. Chem. A* **2002**, *106*, 3445.

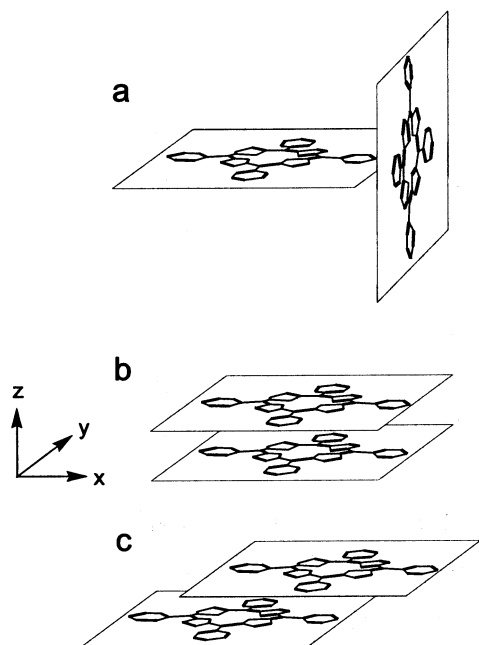


Figure 10. Proposed alignment of neighboring $\text{H}_2\text{TCPP}^{2+}$ molecules in (a) the dimer, (b) the aggregate in HCl , and (c) the aggregate in HNO_3 . The carboxylic acid groups are not shown.

of point charges on the absorption spectra of nonaggregated chlorophyll compounds has been previously shown to lead to spectral shifts of only a few nanometers.³⁷ Thus, it is unlikely that the dramatic spectral differences shown in Figure 2 are a mere consequence of direct interaction of porphyrin monomers with the counterion. In addition, the strong resonance light scattering observed from these samples is evidence that the counterion-dependent spectral perturbations in this pH range are a result of aggregation.

The split Soret band observed at $\text{pH} > 1$ is independent of counterion, and the species which predominates at this pH shows little resonance light scattering. We postulate that a dimer of $\text{H}_2\text{TCPP}^{2+}$ exists between pH 1 and 4. Soret band splittings in covalently linked porphyrin dimers have been reported in the range from about 500 to 1000 cm^{-1} , depending on the relative orientation of the molecular planes.³⁸ The etio pattern in the Q-band region of the putative dimer spectrum is taken as evidence for perturbations to the porphyrin core which lower the symmetry from the D_{4h} symmetry of the diacid monomer, because it is well known that degenerate Q-bands are observed for diacid and metalated porphyrins.³⁹ We propose that the perturbation responsible for Q-band splitting results from hydrogen bonding between $\text{N}-\text{H}^+$ and carboxylic acid groups. Such an interaction would lead to a perpendicular orientation of neighboring molecular planes as shown in Figure 10a. It is unlikely that the symmetry lowering alone is responsible for the Soret band splitting in the dimer. Gouterman⁴⁰ has explained why reduction from four-fold to two-fold symmetry at the porphyrin core leads to a larger splitting of the Q-band than the Soret band. In the next section, we explore whether the observed splitting of the Soret band in the putative dimer spectrum of $\text{H}_2\text{TCPP}^{2+}$ can reasonably be explained in terms of exciton coupling.

To our knowledge, there is little literature precedent for counterion dependence of the spectra of chromophore ag-

gregates. Counterion-dependent shifts of a few nanometers have been reported in the case of J-aggregates of pseudocyanine.⁴¹ The absence of a counterion effect in the case of the $\text{H}_2\text{TSP}^{2-}$ J-aggregate is to be expected if the charge on the porphyrin is balanced by protons, which are of course abundant at low pH. The diacid of TCPP, on the other hand, carries a net positive charge at pH values well below 5 and thus requires nearby negative ions to compensate the charge. Although it is possible that the anions participate directly in the spectroscopic transitions to effect the differences exhibited in Figure 2, a more likely explanation is that the identity of the counterion determines the structure and hence the excitonic coupling in the aggregate.

It is important to consider the role of PVA in the formation and stabilization of these aggregates. The use of polymer templates such as DNA⁴² or polyvinyl sulfate⁴³ to create dye aggregates is well known, so one wonders whether the PVA used here provides such a template for aggregate formation. Our experiments show that the absorption spectra obtained for various forms of TCPP are independent of the presence of PVA in freshly prepared solutions. Addition of PVA merely delays the eventual precipitation of aggregated $\text{H}_2\text{TCPP}^{2+}$ in acid solutions. We suppose that PVA interferes with the mesoscopic structure and prevents "aggregation of aggregates" which would lead to precipitation.

4.2. Exciton Theory. In this section, we explore whether first-order exciton theory can account for the observed perturbations to the Soret band of $\text{H}_2\text{TCPP}^{2+}$. We consider only nearest-neighbor coupling of the Soret band transition moments and neglect any coupling of the Soret and Q-band transitions. Because strong perturbations to the Q-bands are observed, this second assumption is probably not valid, and the ensuing conclusions should be considered to be qualitative. We also neglect direct coupling of the porphyrin and counterion transition moments, which is a reasonable approximation to the extent that the respective excited states are well-separated energetically.

4.2.1. Dimer, pH > 1. The counterion-independent species of $\text{H}_2\text{TCPP}^{2+}$ that exists at pH values above 1 is uncertain, but because we have no evidence for large aggregates, we tentatively assign this to a dimer. Transition dipole coupling within a dimer leads to perturbed excited electronic states with energies and transition moments given by⁶

$$E_{\pm} = E_{\text{mono}} \pm 2V_{12} \quad (1)$$

$$\vec{\mu}_{\pm} = \frac{1}{\sqrt{2}} (\vec{\mu}_1 \pm \vec{\mu}_2) \quad (2)$$

where E_{mono} is the energy of the excited state of the monomer, relative to the ground state, μ_i is the (monomer) transition moment of molecule 1 or 2 in the dimer, and V_{12} is the exciton coupling matrix element. For transition dipole coupling, in the point dipole approximation, this is given by

$$V_{12} = \frac{\mu_{\text{ge}}^2}{r^3} [\hat{u}_1 \cdot \hat{u}_2 - 3(\hat{u}_1 \cdot \hat{r})(\hat{u}_2 \cdot \hat{r})] \quad (3)$$

where μ_{ge} is the magnitude of the monomer transition moment, r is the distance between neighboring molecules, \hat{u}_1 and \hat{u}_2 are unit vectors in the directions of the transition moments of molecules 1 and 2, and \hat{r} is a unit vector in the direction of the line connecting the centers of neighboring molecules. The total

absorption strength for both bands of the dimer is proportional to $2\mu_{\text{ge}}^2$; that is, the total intensity is conserved at this level of approximation. In the case of porphyrins, coupling of both components of the in-plane polarized transition must be considered.

In the following analysis, we assume that the two Soret bands at 440 and 404 nm arise from the same porphyrin species, which we postulate to be a dimer. The existence of a single species at pH 1.2 is suggested by the fluorescence data presented above. In work to be presented in a future publication,⁴⁴ we use two-dimensional correlation spectroscopy to analyze the concentration- and pH-dependent absorption spectrum of TCPP in aqueous nitric and hydrochloric acid. In the dimer regime, we find that the bands at 404 and 440 nm evolve synchronously, which also suggests that they are associated with the same species.

To account for the perturbations to the porphyrin core suggested by the absorption and Raman spectra, we tentatively propose a dimer structure in which neighboring porphyrins are perpendicularly oriented as shown in Figure 10a. The coupling of the y -polarized transition moments leads to both red- and blue-shifted excited states. Taking V_{12} to be positive (parallel alignment of $\vec{\mu}_{1,y}$ and $\vec{\mu}_{2,y}$), we find the red-shifted state carries no oscillator strength, while the blue-shifted state has a transition moment which is $\sqrt{2}$ larger than the monomer transition moment. Coupling of the x -polarized transition moment of the molecule on the left with the z -polarized transition moment of the molecule on the right leads to a pair of degenerate dimer states which have the same energy as the monomer ($V_{12} = 0$), each having a transition moment which is equal to the monomer value μ_{ge} . This model leads to the prediction of two bands of equal intensity, one blue-shifted and one unshifted from the monomer transition. The predicted energy level scheme for the dimer model is in qualitative agreement with our observations: absorption maxima at 404 and 440 nm (with a shoulder at 439 nm). However, the relative intensity of the two bands varies with pH, because of the overlap with the monomer feature at 440 nm, so we cannot obtain the inherent relative intensities of the two dimer bands. The synchronous decrease in all of these features (404, 439, and 404 nm) as the pH is lowered or concentration increased is the result of converting both monomers and dimers to aggregates.

In the proposed dimer model, the blue shift of $\sim 2200 \text{ cm}^{-1}$ of the peak at 404 nm can be equated to V_{12} . From the integrated absorbance of the diacid in ethanol, we obtained $\mu_{\text{ge}} = 11.7 \text{ D}$ for the monomer transition moment, consistent with an oscillator strength of 1.45, for the degenerate Soret band. Using this value in eq 3 and taking the relative orientations from Figure 10a, we calculated V_{12} to be about 2200 cm^{-1} if the distance between the molecular centers is $\sim 7 \text{ \AA}$. This is somewhat smaller than the $\sim 11 \text{ \AA}$ distance from the center of the porphyrin ring to the edge of the $-\text{COOH}$ group,^{16,25} but the qualitative agreement with experiment lends support to the model. However, rather large perturbations to the π electron framework are suggested, and the simple perturbation theory approach on which eqs 1–3 are based is probably inadequate. We conclude that the proposed dimer model is reasonable but should be considered tentative.

4.2.2. Aggregates, pH < 1. The above approach is now extended to the consideration of exciton coupling among N molecules, where N is the aforementioned coherence number.

The energy and transition moment for the transition from the ground to the k th exciton state are given by⁵

$$E_k = E_{\text{mono}} + 2V_{12} \cos\left(\frac{k\pi}{N+1}\right) \quad (4)$$

$$\mu_{\text{gk}} = \mu_{\text{ge}} \sqrt{\frac{2}{N(N+1)}} \left(\frac{1 - (-1)^k}{2} \right) \cot\left[\frac{k\pi}{2(N+1)} \right] \quad (5)$$

where k is an integer ranging from 1 to N , and μ_{ge} and V_{12} are as defined above. Equations 4 and 5 neglect disorder and nonnearest neighbor couplings.

On attempting to apply these equations to the aggregate which forms in HCl solution, we have to explain the existence of a single blue-shifted aggregate transition. The increased width (1840 cm^{-1} , fwhm) of the aggregate Soret band as compared to that of the monomer (980 cm^{-1}) hints at the possibility that the aggregate absorption in HCl is a superposition of two overlapping bands or that a random distribution of relative orientations of monomers leads to a broadening of the absorption band. Indeed, broadening of the Soret band in porphyrin aggregates is well known (see, for example, ref 32), and the occurrence of a sharp J-band is relatively rare. The absence of structure in the Q-band region of the HCl (or HNO_3) aggregate argues against the possibility that the aggregate is built up from dimer units oriented as discussed above. If only a single exciton state at 417 nm exists, this is consistent with an aggregate in which the porphyrin planes are stacked vertically like plates (an H-type aggregate) as shown in Figure 10b, preserving the local four-fold symmetry and leading to an allowed blue-shifted transition and forbidden red-shifted transition. For this geometry, the angular factor in eq 3 is unity, and V_{12} is equal to μ_{ge}^2/r^3 . Given the apparent lack of exchange narrowing, we put N equal to 2 in eq 4 and equate the 1300 cm^{-1} blue shift with V_{12} to find an approximate distance of 8 \AA between neighboring molecules in the HCl aggregate. This is considerably larger than the typical van der Waals separation of about 3.5 \AA observed in π stacking of neutral aromatic compounds. Given that the ionic diameter of Cl^- is about 3.4 \AA , we speculate that the chloride ions intercalate between porphyrin planes in the aggregate. Hydrogen bonding between Cl^- ions and the $\text{N}-\text{H}^+$ groups of porphyrin diacids has been detected crystallographically,¹⁶ and the distance between N and Cl was found to be about 4 \AA . Thus, the qualitative features of the aggregate in HCl solution suggest an H-type structure in which Cl^- ions are sandwiched between neighboring porphyrins.

In the aggregate which forms in nitric acid, on the other hand, the J-band at 467 nm is narrower than the monomer absorption by almost a factor of 2. We thus take the coherence number to be 4 and apply the above equations to find the transition moment coupling V_{12} for the HNO_3 aggregate. From eq 5, the exciton state $k = 1$ carries about 95% of the oscillator strength, and the difference between the monomer and aggregate bands is equal to $1.62V_{12}$. Given the similar characteristics of the TCPP aggregate in nitric acid and the well-studied TSPP aggregates, we propose the stacking arrangement shown in Figure 10c, in which neighboring molecular planes are parallel, but the molecular centers are displaced. Coupling of the transition moments along the x direction (parallel to the aggregate axis) leads to a red-shifted (J-band) exciton state, while coupling of the y -polarized transition moments results in a blue-shifted (H-band)

transition. Using the experimental splittings of the H- and J-bands at 406 and 467 nm, relative to the monomer transition at 440, we predicted the couplings as follows:

$$V_{12}(J) = -800 \text{ cm}^{-1} = \frac{\mu_{\text{ge}}^2}{hcr^3} (1 - 3 \cos^2 \theta) \quad (6)$$

$$V_{12}(H) = 1200 \text{ cm}^{-1} = \frac{\mu_{\text{ge}}^2}{hcr^3} \quad (7)$$

where θ is the angle between the x transition moment and the line connecting the molecular centers. The above equations are satisfied by taking $r \approx 8.3 \text{ \AA}$ and $\theta \approx 42^\circ$, which seem reasonable. The derived interplanar distance again allows for the possibility that anions are intercalated between neighboring porphyrins. It is not necessary to postulate the existence of two different kinds of aggregates to explain the spectrum of TCPP in nitric acid. Because of the degeneracy of the Soret band excited state, both H- and J-bands may result from a single aggregate structure. Polarized absorption studies of flowing samples of $\text{H}_2\text{TSPP}^{2-}$ aggregates¹³ have led to a similar conclusion: the J-band derives from the coupling of transition moments parallel to the aggregate chain, while the H-band results from coupling of the transition moments perpendicular to the chain.

It is not clear why the exchange narrowing of the H-band (which has the same width as the monomer diacid Soret band) is less than that of the J-band. This effect is also observed in aggregated $\text{H}_2\text{TSPP}^{2-}$. Exchange narrowing is opposed by disorder. If indeed there is more disorder (i.e., tilting) of the molecular planes in directions perpendicular to the aggregate axis, then the H-band would experience more inhomogeneous broadening than the J-band. This is clearly only a speculation, and further studies of the nature of the line width of H- and J-bands will be important.

The observed perturbations to the Q-bands of the aggregates are not explainable using exciton theory, because the much smaller transition moment in this case would result in only weak exciton coupling. In addition, the clear increase in Q-band intensity in the aggregates, as compared to that of the monomer, argues against first-order perturbations to the spectra from transition dipole coupling. It is highly likely that the Q- and B-bands themselves are coupled in the aggregate, vibronically or otherwise. In view of this, the above explanations of the Soret band exciton splittings should be considered to be qualitative, as there is evidence that aggregate formation is accompanied by considerable perturbations to the porphyrin electronic structure.

4.3. Comparison to TSPP Aggregates. The spectrum of the aggregate of $\text{H}_2\text{TCPP}^{2+}$ in nitric acid is qualitatively similar to that of $\text{H}_2\text{TSPP}^{2-}$ in acid solution, but the J-band is more red-shifted and shows more exchange narrowing in the latter. Given similar structures for both aggregates, this suggests that the coupling is stronger in the $\text{H}_2\text{TSPP}^{2-}$ aggregate, either because of closer association of the monomer units or because of a larger monomer transition dipole moment. The transition moment for the Soret band of $\text{H}_2\text{TSPP}^{2-}$ monomer is only slightly larger than that of $\text{H}_2\text{TCPP}^{2+}$ (12.6 versus 11.7 D, from the integrated absorbance), so the major effect is assumed to be closer association of porphyrin units in TSPP than in TCPP aggregates.

It is possible that the intervening negative counterions in the case of $\text{H}_2\text{TCPP}^{2+}$ are responsible for this difference. In addition, the zwitterionic nature of the $\text{H}_2\text{TSPP}^{2-}$ monomers contributes a Coulombic stabilization of the aggregate structure which would be less important for the $\text{H}_2\text{TCPP}^{2+}$ system, because the peripheral carboxylic acid groups are uncharged. It has been postulated that a zwitterionic state is a prerequisite to the formation of porphyrin J-aggregates, but the results presented here suggest this is not necessarily so.

4.4. Low-Frequency Raman Modes. As has been observed in previous studies of porphyrin aggregates, low-frequency features are strongly enhanced in the aggregate spectra relative to the monomer. Various explanations of this enhancement have been offered in the literature. Akins et al.²² observed strong bands at 242 and 316 cm^{-1} in the resonance Raman spectrum of TSPP at low pH. These were assigned to the out-of-plane motion of the pyrrolic nitrogens in two different kinds of aggregates. Kano et al.,⁴⁵ who assigned these same vibrations to ruffling and doming motions, respectively, observed coherent oscillations in the sub-5-fs spectroscopy of TSPP J-aggregates at the frequency of the ruffling mode (244 cm^{-1}), but not at that of the doming mode. They attributed the oscillations to modulation of the transition moment through vibronic coupling of the B- and Q-bands via the ruffling motion. Chen et al.²³ used time-dependent theory to model the resonance Raman and absorption spectra of monomeric and aggregated $\text{H}_2\text{TSPP}^{2-}$. They also note enhancement of low-frequency modes of the aggregate when the Raman spectrum is excited at wavelengths within the sharp J-band, but not when the incident wavelength is resonant with the H-band. They associate the enhancement of low-frequency vibrations to the narrowing of the resonant absorption band, a conclusion which is consistent with RR theory and is supported by the good agreement between observed and calculated spectra (both absorption and resonance Raman) reported in ref 23. Enhancement of low-frequency vibrations has also been observed in the *off*-resonance Raman spectra of cyanine dye J-aggregates.³⁵ Recently, Jeong et al.⁴⁶ reported RR spectra of covalently linked zinc(II) porphyrins in which the near neighbor molecular planes are perpendicularly oriented. When the Raman spectrum was excited within the red-shifted excitonic transition (which is not appreciably exchange narrowed), they observed increasing enhancement of low-frequency Raman modes with increasing number of monomers in the array.

Clearly there are many literature examples of aggregation-induced enhancement of low-frequency Raman modes. In this work, however, we found that the out-of-plane porphyrin modes are also quite intense in the *monomer* diacid. Sorting out the enhancement effects associated with aggregation will require measurement of resonance Raman intensities at wavelengths spanning the respective absorption bands. Work along these lines is in progress. The overall resonance Raman intensities, not just those of low-frequency modes, appear to be larger in the aggregate than in the monomer when the detuning of the excitation wavelength is comparable. This appears to be an example of the aggregation-enhanced Raman effect predicted theoretically by Akins.³⁴

(46) Jeong, D. H.; Yoon, M.-C.; Jang, S. M.; Kim, D.; Cho, D. W.; Yoshida, N.; Aratani, N.; Osuka, A. *J. Phys. Chem. A* **2002**, *106*, 2359.

5. Summary

Counterion-dependent excitonic spectra of porphyrin aggregates of $\text{H}_2\text{TCPP}^{2+}$ are reported for the first time. Depending on pH and the nature of the counteranion, $\text{H}_2\text{TCPP}^{2+}$ adopts of number of noncovalently bonded aggregate structures with very different visible absorption spectra. The observed spectral perturbations are qualitatively explained using exciton theory, but quantitative aspects suggest rather strong perturbations to the electronic structure that go beyond the limits of simple first-order exciton coupling theory. This system offers the exciting

possibility that the optical properties in such systems can be tuned by varying the nature and concentration of inorganic counterions in solution.

Acknowledgment. The support of the National Science Foundation is gratefully acknowledged. We thank Prof. Richard Williams for helpful discussions concerning the NMR spectra, and Prof. Ray von Wandruszka for the use of his fluorimeter.

JA0274397